Design of Dual-Output Alternators with Switched–Mode Rectification

Gimba Hassan
Laboratory for Electromagnetic
And Electronic Systems
Massachusetts Institute of Technology
Cambridge MA 02139
Email: gimbah@mit.edu

David J. Perreault
Laboratory for Electromagnetic
And Electronic Systems
Massachusetts Institute of Technology
Cambridge MA 02139
Email: djperrea@mit.edu

Thomas A. Keim
Laboratory for Electromagnetic
And Electronic Systems
Massachusetts Institute of Technology
Cambridge MA 02139
Email: tkeim@mit,edu

Absract-- The push to introduce dual-voltage (42V/14V) automotive electrical systems necessitates power generation solutions capable of supplying power to multiple outputs. A number of approaches for implementing dual-voltage electrical systems have been proposed, but most suffer from severe cost or performance limitations. This paper explores the design of alternators incorporating dual-output switched-mode rectifiers. The proposed approach enables the full load-matched power capability of the alternator machine to be achieved, with power delivered to the two outputs in any desired combination. Switched mode rectifier (SMR) topologies for this application are introduced. Alternator/SMR design guidelines are established, and appropriate control laws are derived. Simulation and experimental results are presented that demonstrate the feasibility and high performance of the approach.

I. INTRODUCTION

Electrification of many automotive functions and the introduction of new features are dramatically increasing the electrical power requirements of vehicles. Functions including electrically powered pumps and valves, and amenities such as heated windscreens and seats, entertainment electronics and navigational aids are driving up the electrical power demand in vehicles [1,6,18]. The increasing power demands are becoming very challenging within the context of the present 14V electrical system and have sparked investigation of higher-voltage electrical systems. The introduction of a 42V electrical system for future automobiles is gaining widespread industry acceptance [6]. Power generation solutions capable of supplying power to two separate buses (e.g. 14V, 42V) are thus becoming important for future vehicles.

Various architectures have been proposed for implementing dual-voltage electrical systems [1,3,5, 6,7,8,10,11,14,15]. Architectures under consideration in the automobile industry include dc/dc converter based architectures and dual–voltage alternator architectures.

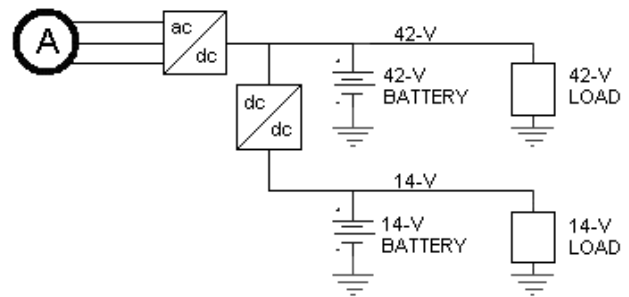In a dc/dc converter-based architecture (Fig. 1), a conventional alternator generates 42V and supplies the 42V

Fig. 1. Dc/dc converter based architecture.

bus. The 42V dc is further processed by a dc/dc converter to supply the 14V bus.

The design of dc/dc converters is relatively well understood, and such converters can achieve very good performance. Nevertheless, dc/dc converters for this application are extremely expensive by automotive standards, and are significantly larger than desired. As a result, this architecture is technically viable (and is likely to be used in the short term) but is probably not economically advantageous over the long term.

An alternative approach is the introduction of an alternator that can directly supply multiple outputs [2,3,5,8,10,11]. Possible dual-output alternators include dual-wound alternators (Fig. 2), and dual-rectified alternators (Fig. 3).

Fig. 2 illustrates the structure of a dual-wound alternator. In this topology, the alternator has two separate sets of stator windings, each supplying an output via a rectifier. In one possible implementation, the 42V bus is supplied by one winding via a diode bridge rectifier, while the 14V bus is supplied by the other winding via a phase-controlled rectifier [3]. The two outputs are controlled by a combination of field control and phase control. The fact that field control is common to both outputs poses serious difficulties in fully regulating both outputs, and in achieving good use of the alternator machine power capability under all operating conditions.

The dual rectified alternator (Fig. 3) comprises an alternator machine with a single winding and a dual-output
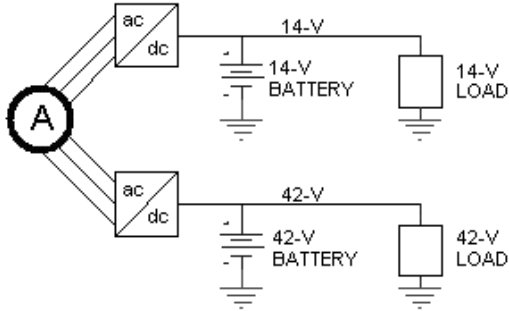
Fig. 2. Dual-wound alternator architecture.

rectifier to supply both the high and low voltage buses. One implementation approach that has been explored in the past [3,8,10,11] is illustrated in Fig.4.

In the implementation of Fig. 4, a conventional diode bridge rectifier is used to supply the 42V bus. The 14V bus is supplied through a semi-controlled rectifier made of three additional thyristors in conjunction with the bottom diodes of the diode bridge. The two outputs can be regulated by a combination of field current and phase control. This approach has been shown to have major limitations [2,3,10]. One limitation is that it is difficult to optimize the machine to be well utilized under different loading conditions. Furthermore, extremely large output filters are required due to the very large, low frequency current ripple appearing at the outputs. The frequency of this ripple is a small multiple of the low alternator electrical frequency and occurs as the thyristors chop current between the outputs.

This paper explores the design of dual-rectified alternators incorporating Switched-Mode Rectifiers (SMR). The design and control approach explored here overcomes the limitations of previous dual-output alternators. Section II of the paper introduces a new class of dual-output switched-mode rectifiers that are suitable for this application, and derives appropriate alternator/SMR control laws. Design guidelines for the alternator and switched-mode rectifier are established in section III. Section IV presents simulation results based on the proposed models and controls. Design of a prototype system and the description of the experimental setup is
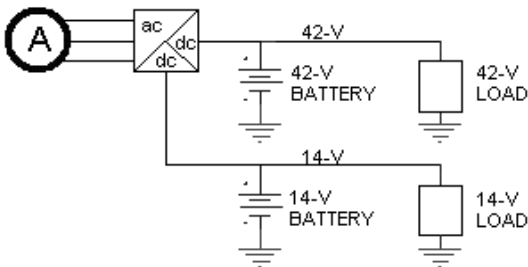

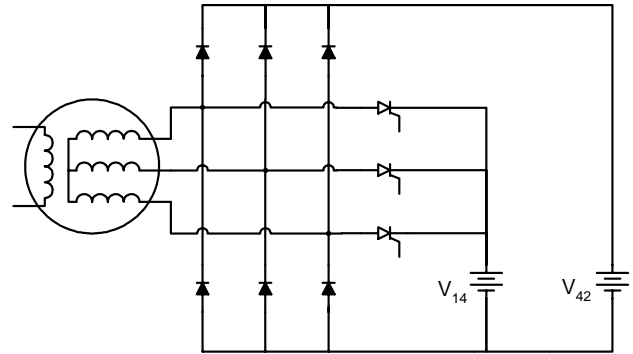**Fig. 3.** Dual rectified alternator architecture.

Fig. 4. Dual rectified alternator with phase-controlled rectifier.

presented in section V. Section VI discusses the experimental results from the prototype system. These results demonstrate the feasibility and high performance of the approach. Finally, section VII concludes the paper.

II. A NEW DUAL-OUTPUT ALTERNATOR

Here we introduce the new alternator design and control laws for it. We consider Lundell-type alternators as these machines are extremely inexpensive and almost universally used in automotive applications. The Lundell machine is a wound-field synchronous machine, and hence has field current i_f as a control input. In developing alternator designs and control laws we adopt the simplified models for such systems developed in [2,5,9,16]. As shown in Fig. 5, the alternator is modeled as a three-phase set of back emf voltages, each in series with an inductance L_s. A diode bridge rectifies the alternator output into a constant voltage load v_x.

Based on the results of [9,16], the alternator output power P_{out} can be calculated as

$$P_{out} = \frac{3V_x}{\pi} \sqrt{\frac{V_s^2 - \left(\frac{2V_x}{\pi}\right)^2}{\omega^2 L_s^2}} \qquad (1)$$
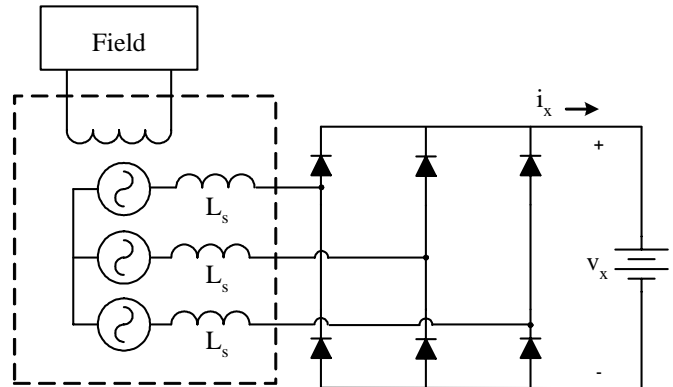

Fig. 5. A simple Lundell alternator model.

where V_x is the output voltage, V_s is the line to neutral back emf magnitude, ω is the alternator electrical frequency, and L_s is the armature synchronous inductance. Computing the back emf voltage as $V_s = k\omega i_f$ (where k is the machine constant in V-s/(rad-A) and i_f is the field current), this can be written as

$$P_{out} = \frac{3V_x}{\pi}\sqrt{\frac{(k\omega i_f)^2 - \left(\frac{2V_x}{\pi}\right)^2}{\omega^2 L_s^2}} \tag{2}$$

To find the load matching condition where output power is maximized,[1] (2) is differentiated with respect to V_x and equated to zero :

$$\frac{\partial P_{out}}{\partial V_x} = \frac{3}{\pi}\sqrt{\frac{(k\omega i_f)^2 - \left(\frac{2V_x}{\pi}\right)^2}{\omega^2 L_s^2}} - \frac{3V_x}{2\pi}\left(\frac{(k\omega i_f)^2 - \left(\frac{2V_x}{\pi}\right)^2}{\omega^2 L_s^2}\right)^{-\frac{1}{2}} \frac{8V_x}{\pi^2 \omega^2 L_s^2} = 0 \tag{3}$$

This can be solved for the load-matched operating voltage :

$$V_x = \frac{\pi k\omega i_f}{2\sqrt{2}} \tag{4}$$

Thus in the load-matched case, we find an average output current of

$$\langle i_x \rangle = \frac{3ki_f}{\sqrt{2\pi L_s}} \tag{5}$$

which results in a load-matched alternator output power of

$$P_{out} = \frac{3k^2 \omega\, i_f^2}{4L_s} \tag{6}$$

Thus, (4) specifies an output voltage for load-matching that results in output power (6). These results will be used to developed dual-output rectifiers that achieve load-matched operation.

A.. *Rectifier topology and operation*
Figure 6 introduces the new dual-output switched-mode rectifier that we use in our design. Alternative implementations having similar operating characteristics are illustrated in Fig. 7(a-c). For clarity we analyze the simpler structure of Fig. 7(c); the rectifier of Fig. 6 operates similarly, but has the rectification and modulation functions integrated into a single stage. To understand the operation of the proposed system, consider the modulation strategy illustrated in Fig. 8. The switching frequency is far higher than the alternator electrical frequency, so alternator phase currents (and rectifier current i_x) may be considered constant during an
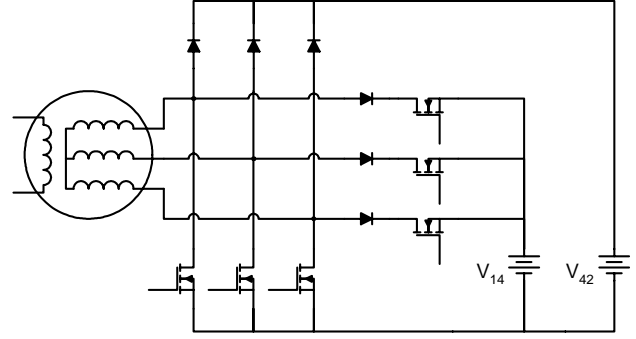
---

[1] That is, the fixed load voltage V_x for which maximum alternator output power is achieved

Fig. 6. The new dual-output switched-mode rectifier.

individual switching cycle. Furthermore, the alternator current i_x is developed based on the local average (over a switching cycle) of the voltage v_x.

Each switching cycle can be broken up into three time segments: In the first segment, which we denote as being hrT in length, the diode D_3 conducts delivering the rectified alternator current i_x to the 42V bus. In the second time period, which lasts for $h(1-r)T$, Q_2 is switched on. In this period diode D_2 and switch Q_2 conduct, delivering the rectified alternator current i_x to the 14V bus. In the final time period, lasting $(1-h)T$, switch Q_1 conducts and the current i_x is shunted to the return bringing the voltage v_x to zero. (See waveforms "A" "D" and "E" of Fig. 8).

Equations for the average rectified bridge voltage $<v_x>$ and the average output currents $<i_{42}>$ and $<i_{14}>$ are derived from waveforms A, D and E in Fig. 8:

$$<v_x> = hrV_{42} + h(1-r)V_{14} \tag{7}$$

$$< i_{42}> = hr\, i_x \tag{8}$$

$$< i_{14}> = h(1-r)\, i_x \tag{9}$$

where
v_x , i_x are the instantaneous alternator voltage and current at the diode bridge output;
V_{14} , i_{14} are the instantaneous voltage and current at the 14V bus;
V_{42} , i_{42} are the instantaneous voltage and current of 42V bus; and "h" and "r" are switch time controls expressed as fractions.

B. *Alternator Control Law*
Here we consider a control law for the alternator and dual-output switched-mode rectifier of Fig 7c. Given desired (reference) output currents i_{14}^* and i_{42}^*, the controls specify the control handles $h, r,$ and i_f such that the desired output currents are achieved. In the event that the desired power exceeds the output capability of the alternator for a given operating point, the alternator should deliver the maximum power possible, with output currents in the desired
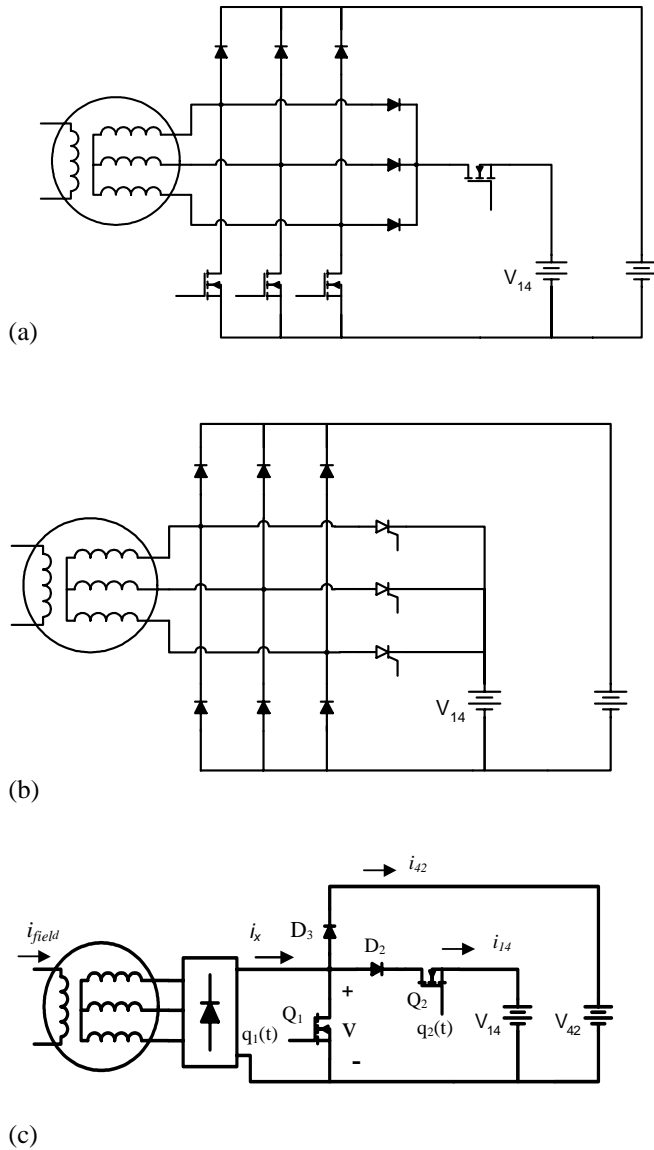
(a)

(b)

(c)

Fig. 7. Alternative rectifier implementations.

proportion. Furthermore the control laws should guarantee that the maximum power capability of the alternator for a given operating point can be achieved.

From (6) the field current is expressed as

$$i_f = \sqrt{\frac{4L_s P_{out}}{3k^2\omega}} \qquad (10)$$

we also have $P_{out} = P_{14} + P_{42} = V_{14}i_{14}^* + V_{42}i_{42}^*$ where i_{14}^*, i_{42}^*, are the desired currents on the 14V and 42V buses, respectively.

As described below, control laws meeting these requirements are given as follows:

$$i_f = \sqrt{\frac{4L_s}{3k^2\omega}(V_{14}i_{14}^* + V_{42}i_{42}^*)} \qquad (11)$$

$$r = \frac{i_{42}^*}{i_{14}^* + i_{42}^*} \qquad (12)$$

$$h = \frac{\pi k\omega i_f}{2\sqrt{2}(rV_{42} + (1-r)V_{14})} \qquad (13)$$

where i_f, r, h are the control handles, i_{14}^*, i_{42}^*, are the current commands (references), and k is the machine constant in *V-s / rad-A*

L_s is the machine synchronous inductance in Henrys
ω is the alternator electrical frequency in *rad/ sec.*

Equation (11) is based on the load-matched power capability derived in (6). It sets the field current i_f to that required for the desired output power (equal to $V_{14}i_{14}^* + V_{42}i_{42}^*$) up to the maximum permissible level. (12) picks the fraction *"r"* such that the currents at the two outputs are in the desired proportion. *"r"* is the fraction of time i_x is delivered to the 42V bus as compared to the time it is delivered to either the 14V or 42V bus. Choosing *"r"* directly in this fashion guarantees that the output currents will remain in the desired proportion even if the total desired output power is not achievable. Finally, time fraction *"h"* in (13) is selected to maintain the load matched condition on the alternator (or as close to it as possible) such as that the full power capability of the alternator can be achieved under any operating condition. (13) follows directly from a combination of the required load-matched voltage $V_x = <v_x>$ (4) and that imposed by the control (7).

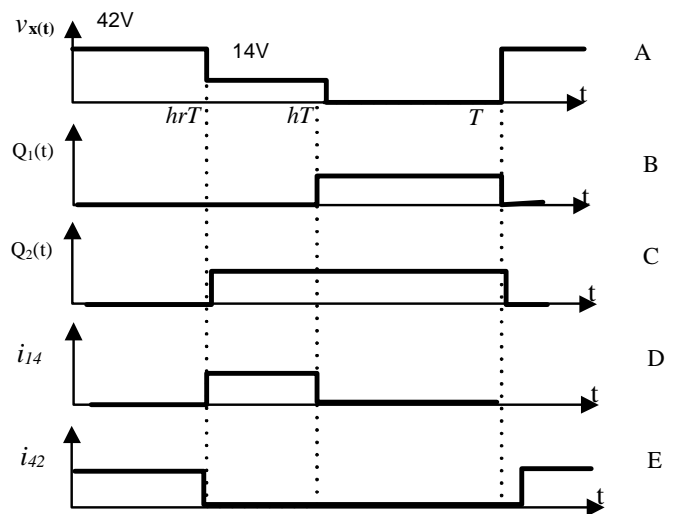**Fig 8.** Circuit waveforms over a switching cycle. (A):voltage v_x, (B): Q_1 gate signal (C): Q_2 signal, (D): i_{14} and (E): i_{42}.

1995

III. DESIGN CONSIDERATIONS AND TRADEOFFS

The alternator machine parameters, (e.g., k, L_s, and R_s) depend on the machine geometry and how it is wound. Machine winding in part reflects a choice between many turns of small wire vs. fewer turns of large wire. Since the SMR control range depends on the parameters mentioned above, the alternator winding selection produces a tradeoff between the power capability at the two outputs vs. speed and the ratings of the rectifier devices. It may be desirable to wind the alternator in such a way that maximum available load-matched power can be delivered to either output. However achieving this capability heavily impacts SMR device sizing. To illustrate this tradeoff, Fig. 9 shows graphs of device and output current ratings versus the normalized number of stator winding turns for a conventional 120 A, 14V alternator geometry. (The winding normalization is such that 1 represents the number of turns on a conventional 120 A, 14V alternator design.).

It can be seen that at idle speed, there is no remarkable change in the output current capability at the two buses with variation in number of stator winding turns. This is also true for the 42V current capability at cruising speed (up to a normalized number of winding turns of approximately 0.8.). There is a great variation, however, in the output current capability at the 14V bus at cruising speed and in the RMS current rating of the boost switch as the number of stator winding turns varies. Achieving full load-matched power capability into the 14 V bus at cruising speed requires a greatly reduced number of winding turns (~ 0.3 normalized). This capability is achieved only at greatly increased current rating of devices Q_1 (shown) and Q_2 (which tracks I_{14}). This trend makes sense: if the alternator is to be able to direct full matched power to either output under all conditions, the machine must have a loa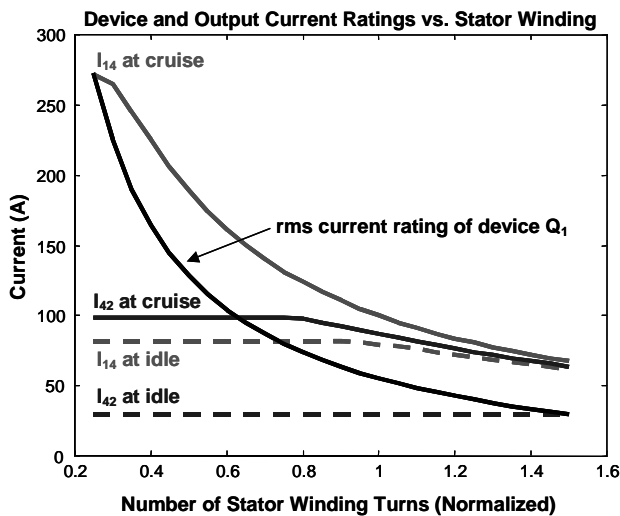d matched voltage below 14 V under all conditions, and the SMR must operate over a wide boost range to direct load-matched power to either output. This results in a high rating of the SMR devices.

As full load-matched capability at cruising speed is not likely to be needed, an intermediate design that cannot direct full load-matched power to either bus under all conditions may be more desirable in view of rectifier component ratings. For most practical designs, normalized winding turns in the range of 0.7 – 1 may be desirable, as it enables full power delivery under idle-speed conditions to either bus, and full power delivery to the 42-V bus under any condition, while preserving low rectifier device ratings. The graph of Fig. 9 (or a similar one for an alternator geometry of choice) may be utilized to evaluate this tradeoff.

IV. SIMULATION RESULTS

Simulations of the averaged model and a circuit model were performed using Matlab and Pspice respectively to determine the performance of the circuit under certain values of the machine parameters.

The parameters for the alternator used for the simulations are given as follows:

$R_s = 0$ (The actual value is ~ $33\, m\Omega$, but is neglected to enable the simplified equations to be used)

$L_s = 135$ µH (The actual value is closer to 105µH, but increased to compensate for neglected stator resistance)

$k = 0.004$ v-s/(rad)A

f, the electrical frequency of the alternator voltage is computed using:

$$f = \frac{P}{2}\frac{rpm}{60} \tag{14}$$

where P is the number of poles (12) and *rpm* is the alternator's speed in revolutions per minute(rpm):

f= 180 Hz, 600 Hz for idle (1800 rpm) and cruising (6000 rpm) speeds respectively.

i_f, the field current for this alternator (named alternator-A), is set not to exceed 3.6 amps.

$f_{sw} = 100$ kHz (SMR switching frequency)

The characteristics of the Alternator/SMR system were first investigated analytically with Matlab, using the averaged equations developed in Section II. The simulations were performed for idle speed (1800 rpm), and cruising speed
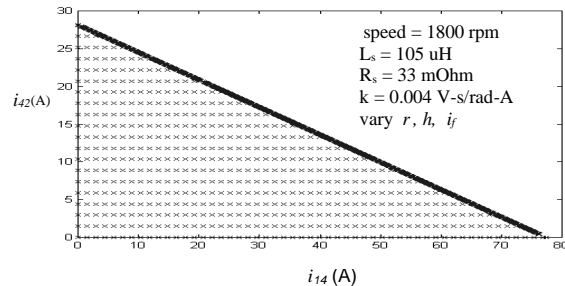
Fig. 9. Tradeoffs in alternator performance and device sizing vs. alternator winding.

Fig. 10. Simulated alternator output over the control range at 1800 rpm.
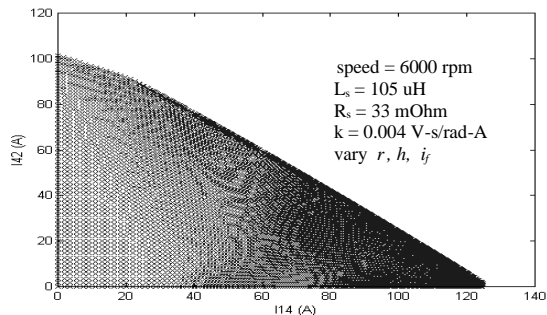
Fig. 11. Simulated alternator output over the control range at 6000 rpm.

(A)

(B)

Fig. 12. Pspice simulation results. (A) Comparison of performance at idle speed and full field with actual and simplified machine parameters. (B) Comparison of performance at idle speed and full field with ideal devices and with device drops modeled.

(6000 rpm), using the machine parameters indicated. Matlab results obtained from varying the control handles r and h at $i_f = 3.6A$ are illustrated in Fig 10 for idle machine speed, and in Fig. 11 for cruising speed. The hatched regions of Figs. 10 and 11 represent achievable operating points of the simulated alternator. These show that it is possible to obtain any desired combination of bus currents, within machine capability, by selecting the appropriate control handles r, h and i_f.

In the Pspice simulations, the effects of stator resistance and device drops were investigated. Two values of stator resistance and inductance were considered, corresponding to actual and approximate machine characteristics. (For simplicity, the control equations assume zero stator resistance. The machine inductance is increased slightly to model the impedance associated with the neglected resistance.) Fig. 12a contains the results for the Pspice simulations with actual (including resistance) and simplified machine parameters. The results indicate that the simplification used to develop the control equations is acceptable. The effect of device drops can be seen in the Pspice simulation results illustrated Fig. 12b. It can be seen that one effect of the device drops is to reduce the achievable current at the 14V output as compared to theoretical calculations. The impact on the 42V output is much lower.

V. EXPERIMENTAL SETUP

Here we describe the prototype system that was developed to validate the proposed approach.

A. Experimental Alternator and Drive Stand

The setup for the experiment is based on a standard Lundell automotive alternator (14 V, 65/130 A) that is driven by a computer controlled variable-speed drive (13.4 kW). For the purpose of this experiment, the internal alternator field regulator and the full bridge rectifier were disabled. An external constant-current power supply is instead connected to the field winding to supply the needed field current. Electronic loads, each with electrolytic capacitor banks (40000 μF, 50VDC) form the constant-voltage loads to represent the batteries of a real system. The SMR outputs are connected to the electronic loads. The capacitor banks are connected to absorb any ripple at the outputs. Current probes
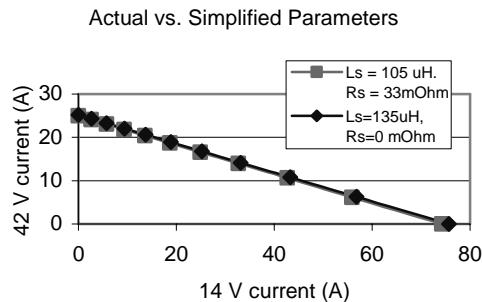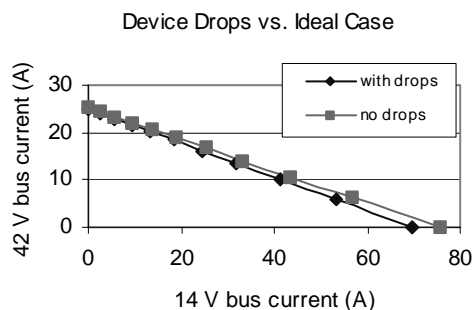
are connected to measure the currents in the buses and are connected to the oscilloscope through the current amplifier. A four-channel oscilloscope is connected for monitoring and measurements of currents, voltages, and gate signals. Pictures of the experimental setup are shown in Figs.13 and 14.

B. Prototype switched-mode rectifier:

The structure of the prototype switched-mode rectifier is shown in Fig. 6. The switches are N-channel MOSFETs (IXYS IXFN230N10). The diodes are each realized using a DSS2x41-01A Schottky Diode Module. The switched mode rectifier also includes multilayer film capacitors across its outputs (ITW Paktron type 106K100V). Nine capacitors are used across the 14 V output, and six are used across the 42 V output. A 16-bit microcontroller C167CR is used to generate the desired pulse-width modulation commands.

VI EXPERIMENTAL MEASUREMENTS AND RESULTS

A. Parameters and control handle calculations

In order to determine the three control handles to be used in the experiment, the control equations developed earlier in Section II are used. We intend to display the capabilities of the experimental apparatus and the operation of the control

Fig. 13. The alternator and motor drive.

Fig. 14. The experimental setup.

Fig. 15 SMR voltage and gating waveforms over a switching cycle.

laws by operating at many combinations of i_{14} and i_{42}. It is convenient to gather and present data in the form of the interrelation between i_{14} and i_{42} when the alternator field current and speed are fixed. To select a matrix of test points, it is convenient to first select a range of values for i_{42}^* to be achieved under the condition $i_{14}^* = 0$. We have selected the following points:

$$i_{42}^*\big|_{i_{14}^*=0} = (31A, 19A, 13A, 9A, 5A, 3A).$$

The corresponding values of i_f are then calculated at idle speed.

The corresponding field currents are:
$i_f = (\ 3.6A, 2.81A, 2.33A, 1.94A, 1.45A, 1.12A\ )$.

For each value of i_f, r is varied from 0 to 1 with step of 0.1. thus

$r = (0, 0.1, 0.2, 0.3, 0.4, 0.5, 0.6, 0.7, 0.8, 0.9, 1)$.

These values of r, i_f are used to determine the values of corresponding control handle h. The calculated values of the control handles i_f, r and h are used in the experiment. The control handle h represents a fraction of the rectifier's fundamental period T. It therefore is limited to values between 0 and 1. Considering the origin of (13), it is apparent that the condition $h>1$ occurs, particularly for large values of i_f and low values of r. A command of $h>1$ reflects a requested power that exceeds the (idealized) alternator capability. h is restricted to the range (0, 1), which will result in the load-matched power if it is achievable, and the maximum power possible in the desired output combination if load-matching is not achievable. It was also found through experimentation and simulation that, particularly at high field currents, a lower h than predicted by the idealized equations results in the best output characteristics. This results from approximations developing the idealized equations (such as neglecting stator resistance and voltage harmonics). To correct for this, the originally-determined values of h are multiplied by 0.8, referred here as the correction factor, which we find gives us very close to the desired performance.

B   Problems encountered

It is worth mentioning that after the alternator's idle-speed performance characteristics were measured for all calculated field currents, the machine stator winding was accidentally destroyed by overloading in an unrelated experiment. This resulted in the use of a second alternator. Thus experimental measurements for the idle and cruising speeds were performed on the newly installed alternator which will henceforth, for easy identification, be referred as alternator-B. The former will be referred as alternator-A. Alternator-B has similar characteristics to alternator-A except that its full-scale field current is approximately 4.2A instead of 3.6A.

C.   Experimental Results

Representative waveforms of voltage v_x (phase-to-ground for one phase) and the gating signals as recorded by the
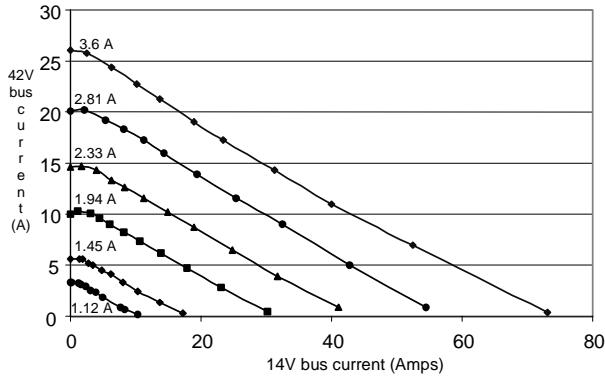
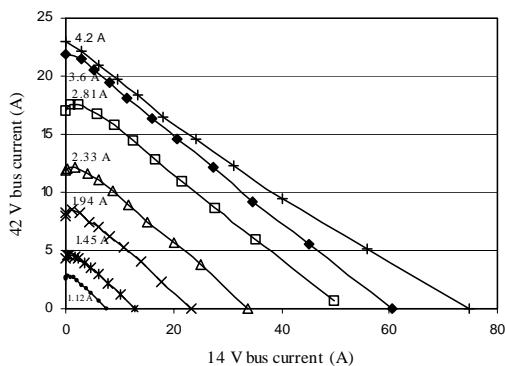**Fig. 16** Alternator-A output currents (1800 rpm).

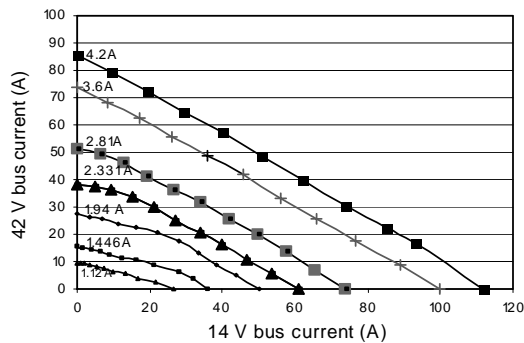**Fig. 17** Alternator-B output currents (1800 rpm).

Fig. 18 Alternator-B output currents (6000 rpm).

oscilloscope are shown in Fig. 15 for a part of the cycle when that phase is delivering current to the output. Experimental results for alternator A(idle speed) are shown in Fig. 16 and the results for alternator B(at idle and cruising speeds) are displayed in Fig. 17 and Fig. 18.

D. Discussion of experimental results

Here we analyze the experimental results. Fig. 16. (alternator-A) and Fig. 17 (alternator-B) show experimental results for idle speed operation of the prototype system over the full output command range. Similar results are illustrated in Fig. 18 for cruising speed operation of alternator-B. These results are consistent with the predicted performance of the system. They demonstrate the ability to achieve the desired system functionality.

Interestingly, the results presented in Fig. 17 and Fig. 18 are for alternator B, a different machine whose parameters may not be exactly the same as the original alternator-A whose parameters were used in determining the control handles. Performance of alternators A and B are very close except that full field current of alternator-B is 4.2 A, rather than 3.6 A for alternator-A. These results both show consistency with expectations, therefore indicating that the SMR technique is easily adaptable to different types of alternators without serious sensitivity to the machine parameters. The experimental results obtained are very much consistent with the results obtained from simulations within the approximations used in developing the system. These results demonstrate the feasibility and high performance of the proposed approached. Thus, the dual-output alternator overcomes the limitations prevailing with other designs as mentioned in Section I. It has been shown that to a reasonable approximation the SMR approach enables the full load-matched power capability of the alternator machine to be achieved at idle speed, with power delivered to the two outputs in any desired combination. At high speeds, the output power capabilities are consist with the alternator design as highlighted in section III

VII CONCLUSION

The push to introduce dual-voltage (42V/14V) automotive electrical systems necessitates power generation solutions capable of supplying power to multiple outputs. A number of approaches for implementing dual-voltage electrical systems have been proposed, but most suffer from severe cost or performance limitations. This paper explores the design of alternators incorporating dual-output switched-mode rectifiers. The proposed approach enables the full load-matched power capability of the alternator machine to be achieved, with power delivered to the two outputs in any desired combination. Switched mode rectifier topologies for this application are introduced, and design guidelines for the Alternator/SMR system are established. An alternator control law is devised that enables full utilization of the machine capability. Simulation and experimental results that demonstrate the feasibility and high performance of the approach are also presented. It is anticipated that the technology proposed here will be of value in future dual-voltage automotive electrical systems.

companies of the MIT/Industry Consortium on Advanced Automotive Electrical/Electronic Components and Systems, which supported this work.

REFERENCES

[1]   J. M. Miller, "Multiple voltage electrical power distribution system for automotive applications," *Intersociety Energy Conversion Conference (IECEC),* Washington, DC, August 1996.

[2]   D.J. Perreault, V. Caliskan, "Automotive power generation and control," *Technical report TR-00-003,* Laboratory for Electromagnetic and Electronic Systems (LEES), MIT, May 24, 2000.

[3]   J. C. Byrum, "Comparative Evaluation of Dual-Voltage Automotive Alternators," *Technical report TR-00-012*, Laboratory for Electromagnetic and Electronic Systems (LEES), MIT. November 6, 2000.

[4]   J.G. Kassakian, J.M. Miller, N. Traub. "Automotive electronics power up," *IEEE Spectrum,* May 2000.

[5]   D.J. Perreault, V. Caliskan. "A new design for Automotive alternators," *2000 International Congress on Transportation Electronics. (Convergence 2000),* pp 583 – 594, October 2000, SAE paper 2000 – 01 – C084.

[6]   J.M. Miller, D. Goel, D. Kaminski, H.P. Schoner, T.M. Jahns, "Making the case for next generation automotive electrical system," *1998 International Congress on Transportation Electronics* (Convergence 1998), October 1998, pp 41 – 51.

[7]   G. A. Williams and M. J. Holt, "The future of vehicle electrical power systems and their impact on system design," SAE Paper 911653, *Future Transportation Technology Conference and Exposition,* Portland, Oregon, Aug. 1991.

[8]   J. Becker, M. Pourkermani & E. Saraie, "Dual-Voltage Alternators," SAE Paper 922488, *International Truck and Bus Meeting and Exposition,* Toledo, Ohio, November 16-19, 1992.

[9]   V. Caliskan., D. J. Perreault, T. M. Jahns, and J. G. Kassakian, "Analysis of Three-Phase Rectifiers with Constant-Voltage Loads," *IEEE Power Electronics Specialists Conference,* Charleston, SC, June 1999, pp. 715-720.

[10]   C. R. Smith. "Review of heavy duty dual voltage systems." SAE technical Paper series, # 911857, *International Off-Highway and Power Plant Congress and Exposition,* Milwaukee, Wisconsin, Sept. 1991.

[11]   J. O. Dwyer, C. Patterson & T. Reibe, "Dual Voltage Alternator." *IEE Colloquium on Machines for Automotive Applications,* Monday, 4 November 1996. pp. 4/1-4/5.

[12]   J. G. Kassakian, "Automotive Electrical Systems – The power Electronics Market of the Future," *Proceedings of IEEE Applied Power Electronics Conference and Exposition (APEC 2000),* vol. 1, pp. 3-9, New Orleans, LA, February 2000

[13]   J. V. Hellmann and R. J. Sandel, "Dual/high voltage vehicle electrical systems," SAE Paper 911652, *Future Transportation Technology Conference and Exposition,* Portland, Oregon, Aug. 1991.

[14]   M. F. Matouka, "Design considerations for higher voltage automotive electrical systems," SAE Paper 911654, *Future Transportation Technology Conference and Exposition,* Portland, Oregon, Aug. 1991.

[15]   S. Muller and X. Pfab, "Considerations implementing a dual voltage power network," SAE Paper 98C008, *IEEE-SAE International Conference on Transportation Electronics (Convergence),* Dearborn, MI, Oct. 1998.

[16]   V. Caliskan, D. J. Perreault, T. M. Jahns, and J. G. Kassakian, "Analysis of Three-Phase Rectifiers with Constant-Voltage Loads," *IEEE Transactions on Circuits and Systems -I,* (to appear).

[17]   "A New 42-Volt Standard." *Technology Review,* July/August 2002. pp 10-11.

[18]   J. G. Kassakian, H. C. Wolf, J. M. Miller, and C. J. Hurton, *"Automotive Electrical Systems Circa 2005," IEEE Spectrum,* August 1996, pp. 22 –27.